



18F-Fluorodeoxyglucose positron emission tomography with computed tomography (FDG PET/CT) findings in children with encephalitis and comparison to conventional imaging

Sophie Turpin¹ · Patrick Martineau² · Marc-André Levasseur³ · Inge Meijer⁴ · Jean-Claude Décarie⁵ · Julie Barsalou⁶ · Christian Renaud⁷ · Hélène Decaluwe⁶ · Elie Haddad⁶ · Raymond Lambert¹

Received: 27 July 2018 / Accepted: 28 February 2019 / Published online: 12 March 2019
© Springer-Verlag GmbH Germany, part of Springer Nature 2019

Abstract

Purpose FDG PET/CT is emerging as a new tool for the evaluation of acute encephalitis (AE). However, to date, there are no exclusively pediatric studies on the use of FDG PET for suspected AE. The objective of this study was to compare qualitative and quantitative brain PET to conventional brain imaging in a cohort of children, and to identify patterns of metabolic abnormalities characteristic of AE.

Methods This retrospective study included 34 children imaged with PET/CT, CT and magnetic resonance imaging (MRI). The positivity rate of all three imaging modalities was measured. Besides visual assessment, quantification of relative regional brain metabolism (RRBM) was performed and compared to a database of normal pediatric brains.

Results Fourteen subjects had a clinical diagnosis of autoimmune encephalitis (AIE) or encephalitis of unknown origin (EX), six of anti-N-methyl-D-aspartate receptor (anti-NMDAr) encephalitis, three of Hashimoto's encephalopathy, three of neurolyupus and eight had other subtypes of encephalitis.

Quantitative PET was abnormal in 100% of cases, visually assessed PET in 94.1% of subjects, MRI in 41.2% and CT in 6.9%. RRBM quantification demonstrated multiple hyper and hypo metabolic cortical regions in 82.3% of subjects, exclusively hypermetabolic abnormalities in 3%, and exclusively hypometabolic abnormalities in 14.7%. The basal ganglia were hypermetabolic in 26.5% of cases on visual assessment and in 58.8% of subjects using quantification.

Conclusion In our pediatric population FDG PET was more sensitive than conventional imaging for the detection of AE, and basal ganglia hypermetabolism was frequently encountered.

Keywords Fluorodeoxyglucose · Positron emission tomography · Computed tomography · Magnetic resonance imaging · Children · Encephalitis

✉ Sophie Turpin
turpinsop@hotmail.com

¹ Division of Nuclear Medicine, Department of Medical Imaging, Centre Hospitalier Universitaire Sainte-Justine, 3175 Chemin de la Côte-Sainte-Catherine, Montréal, Québec H3T 1C5, Canada

² Department of Nuclear Medicine, Health Sciences Centre, University of Manitoba, Winnipeg, Manitoba, Canada

³ Department of Nuclear Medicine, Centre Hospitalier Universitaire de Sherbrooke, Sherbrooke, Québec, Canada

⁴ Division of Neurology, Department of Pediatrics, Centre Hospitalier Universitaire Sainte-Justine, Montréal, Québec, Canada

⁵ Department of Medical Imaging, Centre Hospitalier Universitaire Sainte-Justine, Montréal, Québec, Canada

⁶ Division of Immunology, Allergy, Rheumatology, Department of Pediatrics, Centre Hospitalier Universitaire Sainte-Justine, Montréal, Québec, Canada

⁷ Division of Microbiology, Infectious Disease, Department of Pediatrics, Centre Hospitalier Universitaire Sainte-Justine, Montréal, Québec, Canada

Introduction

Brain positron emission tomography (PET) associated with computed tomography (CT) using 18F-FluoroDeoxyGlucose (FDG) has played an important role in the pediatric population for the evaluation of epilepsy for many years. More recently, in addition to the evaluation of dementia, auto-immune encephalitis has been emerging as a potential new indication for brain PET imaging in adults. To date, FDG PET brain studies have been almost exclusively performed in adults, the large majority as evaluation of paraneoplastic symptoms. The purpose of our study was to evaluate the role of brain PET in a cohort of children with acute encephalitis in comparison to conventional imaging and to identify, if possible, distribution patterns of brain anomalies associated with specific AE subtypes.

Materials and methods

This retrospective study was approved by our institutional review board and the requirement to obtain informed consent was waived.

Population

A total of 104 pediatric subjects were referred to our institution between April 2008 and February 2018 for dedicated 18F-FDG brain PET/CT for the evaluation of neuro-inflammation. These subjects were identified through our radiological information system. The Emerging Infections Program Encephalitis Project criteria were used for the definition of encephalitis and require the major criterion of altered mental status lasting ≥ 24 h and one or more of the following minor criteria: 1. Fever $\geq 38^\circ\text{C}$ occurring ≤ 72 h before or after hospital admission; 2. Seizures; 3. Focal neurologic deficits not previously present on examination; 4. Cerebrospinal fluid (CSF) pleiocytosis (≥ 5 leukocytes/ mm^3); 5. Abnormal electro-encephalogram (EEG); 6. Abnormal neuroimaging (computed tomography or magnetic resonance imaging) representing an acute process [1].

Subject evaluation

Initial subject evaluation encompassed standard laboratory studies including complete blood count, inflammatory markers (i.e. ESR, CRP), toxicology screening; lumbar puncture if not contraindicated with CSF analysis including cell count, glucose, protein, viral and bacterial culture, opening pressure and more recently oligoclonal bands and polymerase chain reaction (PCR) for Enterovirus (EV), Epstein-Barr virus (EBV), Herpes Simplex Virus 1 and 2 (HSV1 and HSV2) and Cytomegalovirus (CMV). Conventional neuro-imaging (CT

and/or MRI) was also performed. Additional blood work including lupus panel (anti-nuclear antibodies, ANCA, anti-dsDNA ELISA, anti-dsDNA by immunofluorescence, anti-Smith, anti-SM/RNP, anti-Ro/SSA, anti-La/SSB, anti-Histone, anti-JO1, anti-SC170, anti-CENP-B, anti-cardiolipin), rheumatoid factor, TSH and anti-TPO, microbiological evaluation (West Nile, Lyme, Mycoplasma, Zika, Jamestown Canyon, Snowshoe hare, Posawan, Bartonella, Equine, Leptospira, lymphocytic choriomeningitis) and in patients with suspected ADEM, antibodies to myelin oligodendrocyte glycoprotein (MOG), was performed on an individual basis. In both serum and CSF, antibodies evaluation has evolved over the years and there was no standard protocol for all patients. From 2008 to 2014, anti-NMDAR antibodies analysis was performed in an outside facility. Since 2014, anti-NMDAR antibodies have been tested in our institution. Paraneoplastic panels including anti-Hu, anti-Ri, anti-Yo, anti-CV2, anti-PNMA2 and anti-Amphiphysine has been available since 2013 and performed at the McGill University Health Center (Montreal, Canada). Finally, anti-AMPA, anti-VGKC, anti-GABA, and anti-DPPX have been tested since 2014 in an outside facility (Mitogen Advanced Diagnostic Laboratory, Calgary, Canada) [2–8].

Imaging

Computed tomography

Multi-detector scanners were used for computed tomography (CT). Initially, a General Electric VCT Lightspeed 64 Electric was used, which was later replaced by a Siemens Somatom Dual Flash. Spiral acquisitions with 5-mm slices reconstructed in 1-mm slices with a 0.7-mm gap were acquired. Non-ionic iodinated contrast agents were used.

Magnetic resonance imaging

Three devices were used for magnetic resonance imaging (MRI): one General Electric 750 3 Tesla and two 1.5 Tesla scanners (a Siemens Avento and a Philips Ingenia). Standard protocols included sagittal and axial T1 weighted images, axial T2, coronal FLAIR and axial diffusion weighted imaging. Non-ionic Gadolinium based contrast agents were used and 3D T1 weighted sequence was acquired after the injection.

FDG PET/CT

Prior to PET, all subjects fasted for a minimum of 4 h. Dextrose containing intravenous solutions were stopped 2 h before administration of FDG. Blood glucose levels were measured prior to injection to ensure values of ≤ 8 mmol/L.

At the time of diagnosis, all subjects underwent brain studies first, to ensure the completion of the most important part of

the examination as many patients came from ICU, followed by whole-body acquisition. During follow-up, either brain acquisition or the combination of brain and whole-body acquisition was performed according to the clinical context.

PET acquisitions were performed for 45–60 min for brain studies and 60–90 min for head-neck and whole-body examinations, after injection of 3.5–5 MBq/kg of 18F-FDG (minimum 37 MBq). PET/CT was performed using a Philips Gemini 16 time-of-flight PET-CT scanner. Acquisition duration was 10 min/FOV for the dedicated brain acquisition and 2.5 min/FOV for the whole body. CT parameters for attenuation correction were 120 kVp, pitch 0.813, rotation time 0.5 s, slice thickness 5 mm, and collimation 16×1.5 mm. For whole body scanning, CT tube current (mA) was adjusted according to weight: < 45 kg: 22 mA; 46–67 kg: 33 mA; 68–90 kg: 44 mA; > 91 kg: 66 mA and for brain studies 45 mA was used. PET images were acquired in 3D mode and reconstructed using a row-action maximum likelihood algorithm (3 iterations, 33 subsets).

No subjects received sedation for the purpose of PET imaging. As some subjects were receiving sedative medications as part of their medical management, especially in an intensive care setting, medical, nursing and nuclear medicine technologists notes were reviewed to identify timing of medication to FDG injection and the state of consciousness at time of FDG injection. In subjects scheduled for dedicated brain studies, subjects were instructed to rest with minimal auditory and visual stimulation. Subjects were otherwise isolated in a dedicated room during the uptake period in the presence of their family and a television.

Data analysis

For qualitative PET and conventional imaging, anomalies were identified from the radiological report. Visual assessment of PET and conventional imaging was performed by board-certified nuclear medicine specialists and board-certified radiologists respectively who were not blinded to the clinical data. Encephalitis was suspected if there was the presence of multiple focal cortical and/or subcortical anomalies on MRI and hyper and/or hypometabolic foci on qualitative PET, not following a vascular territory and after exclusion of other causes such as metastatic disease. In patients with sedative medication, diffuse and homogenous hypometabolism, without focal anomalies, involving the whole brain on PET was considered as an effect of medication and not encephalitis [9].

Brain PET images were analyzed using NeuroQ™ (Syntermed, Atlanta, United States), a commercially available software package which performs automated quantitative analysis of activity in standardized volumes of interest in the brain. After defining upper and lower limits for the brain, scalp activity was removed using the threshold

set by the program, corresponding to 20% of the image counts. Realignment of slices in three planes (axial, coronal and sagittal) was performed using rigid registration. Ten iterations were used to perform elastic transformation of the patient brain data to the adult normal brain template provided by the NeuroQ™ software. The normal FDG brain database was developed in our institution from a cohort of subjects without neurological anomalies. Pediatric patients referred to our institution between April 2008 and June 2017 for dedicated 18F-FDG brain were identified through our radiological information system. Prospective extraction of brain data from head and neck or whole body PET/CT scans was started in October 2015 until June 2017. In order to minimize the potentially confounding effects of concomitant CNS disease, patient charts were reviewed in order to exclude patients with primary or secondary brain neoplasms, epilepsy, known collagen-vascular disease, neuropsychiatric symptoms (such as depression or psychosis), developmental disabilities such as trisomy 21, previous brain surgery or instrumentation, and patients taking medications known to interfere with brain metabolism or under chemotherapy. Patients did not undergo formal neuropsychological evaluation. After exclusions, we identified 88 normal subjects, 43 males and 45 females, ranging in age from 6 months to 18 years of age. Subjects were assigned to either the development group ($N = 59$) or the validation group ($N = 29$). The development group included 30 boys (9.15 ± 5.6 years) and 29 girls (9.83 ± 4.8 years) and the validation group included 13 boys (8.77 ± 5.4 years) and 16 girls (11 ± 5.4 years). There was no significant difference in age ($p = 0.67$) or gender ($p = 0.59$) between the groups.

Each normal subject's regional relative brain metabolism (RRBM) was automatically quantified in 47 standardized cortical and subcortical volumes of interest, including 22 paired regions. Graphical depiction of NeuroQ brain segmentation for result reporting is found in Fig. 1. Using the NeuroQ™ data from the development group, RRBM relative to age were modeled using multiple linear and non-linear mathematical equations. The significance of gender was assessed using the Student t-test. Optimal models were selected using the Akaike Information Criterion. Mean predicted values and 95% prediction intervals were derived for all regions. In addition to the posterior fossa, RRBM quantification was performed for 12 frontal regions, ten parietal, ten temporal, four occipital and six regions concerning the basal ganglia. An Excel file was created allowing direct transfer of NeuroQ™ data and color coded visualization of results as our software license did not permit the creation of a new NeuroQ™ database. Accuracy of the model predictions was assessed by comparing each normal validation group RRBM to the age and gender matched 95% prediction

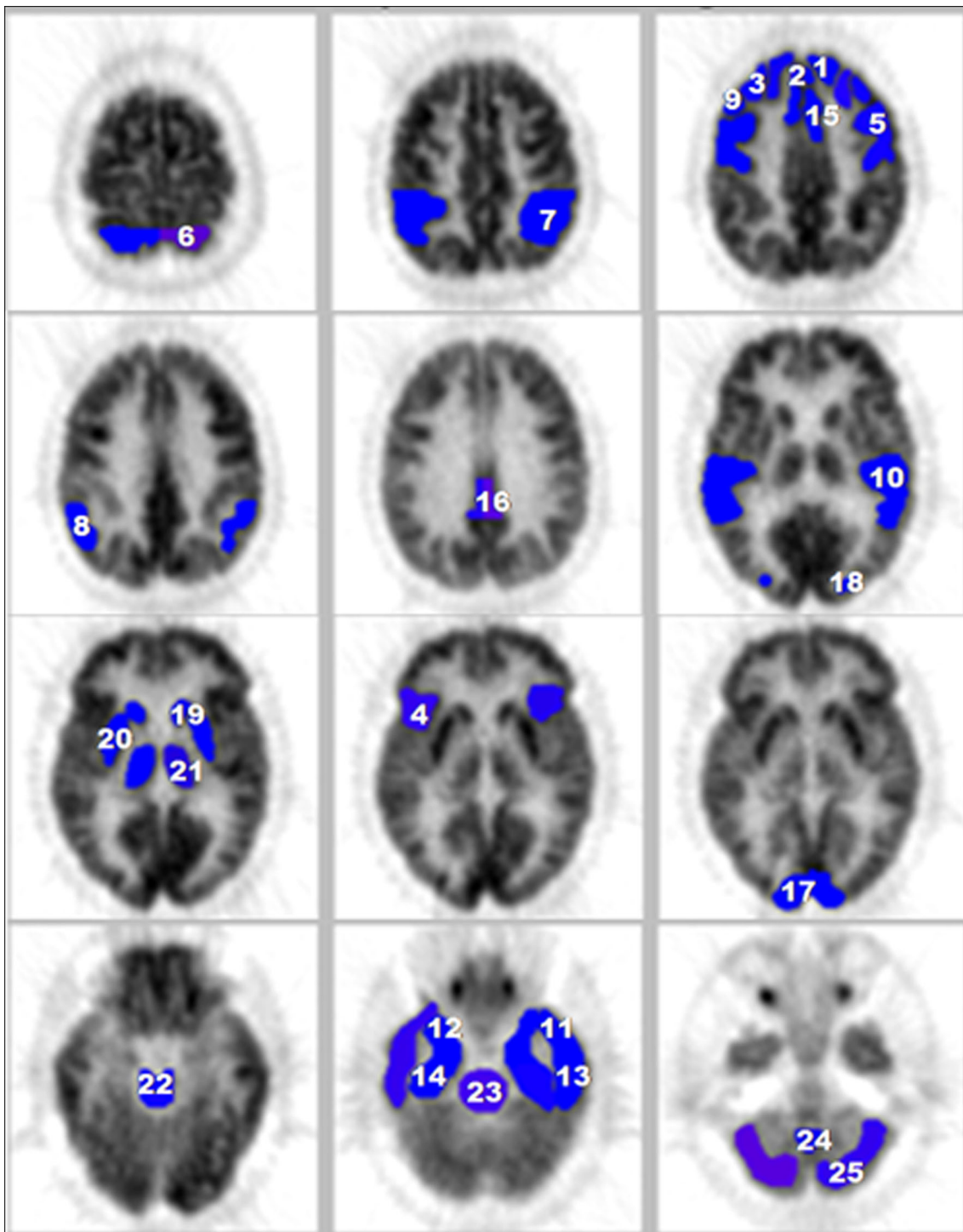


Fig. 1 Overview of brain segmentation in 47 volumes of interest, overlying the normal adult template, for the purpose of graphical representation of NeuroQ™ results (Syntermed, Atlanta, United States). (With permission from Dr Daniel H Silverman). 1: GFs = Superior frontal; 2: GFd = Medial frontal; 3: GFm = Mid frontal; 4: GFi = Inferior frontal; 5: SM = Sensorimotor; 6: sPL = Superior parietal; 7: iPL = Inferior parietal; 8: PTC = Parietotemporal; 9: Broca = Broca; 10: sLT =

Superior lateral temporal; 11: iLAT = Inferior lateral anterior temporal; 12: MAT = Anterior medial temporal; 13: iLPT = Inferior lateral posterior temporal; 14: MPT = Posterior medial temporal; 15: GCa = Anterior cingulate; 16: PCC = Posterior cingulate; 17: PVC = Primary visual cortex; 18: AVC = Associative visual cortex; 19: CN = Caudate nucleus; 20: LN = Lentiform nucleus; 21: Th = Thalamus; 22: MB = Midbrain; 23: P = Pons; 24: V = Vermis; 25: Cbm = Cerebellum

interval established with our mathematical models. Regions of RRBM outside the 95% prediction interval

were considered abnormal. In the validation group, 94.3% of regions fell within the 95% prediction interval

for the whole group and 95.7% of regions for subjects more than 3 years of age [10].

For the present study, each patient's RRBM was compared to the appropriate age and gender mean predicted value and 95% prediction interval. The number of increased regions above the 95% prediction interval upper limit and of decreased regions below the 95% prediction interval lower limit was established for each subject. Due to licensing limitations, NeuroQ output images with color-coded regions depicting the significant regional differences from our custom normal paediatric dataset were not able to be generated within the NeuroQ software package. Therefore, we, the authors, manually recreated regions matching the NeuroQ regions and superimposed them on the NeuroQ PET adult template for clarity of showing regional results of the quantitative comparison. Regions of RRBM within the 95% prediction interval are represented in green, those above the upper limit of the 95% prediction interval in red and those below the lower limit of the 95% prediction interval in blue.

For the entire group of patients with encephalitis the number of regions outside the 95% prediction interval was compared to those of the validation group. Comparison was also made in between the following subgroup: anti-NMDAR encephalitis, Hashimoto's encephalitis, neurolupus and AEI/EX. For the statistical analysis of qualitative findings, a binary approach was used for each lobe and the basal ganglia. A score of 1 was given for the presence of a focal anomaly in a lobe or increased uptake in the basal ganglia and a score of 0 for the absence of a lobar anomaly or basal ganglia hypermetabolism.

Statistical analysis was performed using unpaired t-test (GraphPad Software Online) for comparison between groups. Categorical variables are presented as frequencies, and continuous variables as mean \pm standard deviation (SD). All statistical analyses were two-tailed, and a p value <0.05 was considered significant.

Diagnosis and follow-up

The final diagnosis concerning the etiology of the encephalitis in each patient was obtained from the medical file. Encephalitis was classified according to the etiology: anti-NMDAR, Hashimoto's, lupus, bacterial, or viral. The diagnosis of probable autoimmune encephalitis (AIE) was considered according to clinical, laboratory and imaging findings and after exclusion of alternative causes [4]. In some patients, the final diagnosis was referred to in the medical file as encephalitis of unknown origin (EX) and not AIE. Immunomodulatory treatments were tailored to the clinical presentation and consisted of high dose corticosteroids usually associated with intravenous immunoglobulin and/or rituximab. Plasmapheresis was reserved for more severe cases.

Results

Population

Thirty-four subjects met the criteria for encephalitis (Table 1). There were 14 boys (7.21 ± 4.68 years) and 20 girls (9.65 ± 5.53 years) similar in age of those of the validation group ($p = 0.38$ for boys and $p = 0.51$ for girls). The delay between the onset of the symptoms and the admission in our institution varied from a few hours to a few days (2.5 ± 3.5 days). The delay between the hospital admission and the PET scan varied from a few days to about 3 weeks (6.4 ± 4.5 days). Eighteen patients were imaged within 7 days of admission, 13 between 8 and 15 days and only 3 between 16 and 20 days after admission. Many patients required hospitalization in the intensive care unit and ten patients were receiving corticosteroids at time of PET due to symptom severity. No patient was comatose at time of PET.

Fever was present in ten subjects, seizures in 24, focal neurological deficits in 18, hallucinations in six and personality changes or psychiatric symptoms (excluding hallucinations) in 12. Acute tics were observed in three subjects and new onset of chorea in one.

CSF analysis was performed in 32 subjects showing pleiocytosis in 18, increased protein content in six and decreased in three, increased glucose content in six and decreased in five. CSF PCR, bacterial and viral cultures came back negative for all subjects.

Anti-NMDAR encephalitis was present in six subjects: anti-NMDAR antibodies were identified in the blood of subjects 1, 3 and 5 and in the CSF of subjects 4 and 6. Anti-NMDAR encephalitis was suspected in subject 2 due to clinical presentation. Hashimoto's encephalopathy was present in three subjects, neurolupus in three, AIE and EX in 14 and other etiologies in eight. Subject 17 was classified as viral encephalitis due to brain abnormalities in the hippocampal region on MRI, even though CSF analysis was negative. Subjects 32, 33, and 34 were classified as EX but the last two subjects likely had AIE as they evolved favorably post immuno-modulation. Uptake in the thyroid gland was found in 2 out of 3 subjects with Hashimoto's encephalitis. Patient 6 was the only subject where a neoplasm (ovarian teratoma) was found.

Comparison of visually assessed PET, CT and MRI

Both CT and/or MRI were performed prior to PET. The delay between MRI and PET varied from a few hours to 17 days (4.6 ± 3.7 days). CT was performed in 29 subjects at admission and prior to both MRI and PET. CT was abnormal in two. In subject 12, findings on CT were similar to PET and MRI anomalies and classified as encephalitis. In patient 16, ADEM was demonstrated on both CT and MRI but findings on PET were classified as encephalitis.

Table 1 Patient demographics and diagnosis

Patient number	Gender	Age (years)	Diagnosis	Delay (days)	Clinical findings	Relevant medication at time of PET
1	Male	5	Anti-NMDAr	7	Seizures, Hallucinations, Psychosis	Corticosteroids, Midazolam (1 h30 prior to FDG)
2	Female	18	Anti-NMDAr	12	Seizures, Psychosis	Lorazepam, Anticonvulsants
3	Female	17	Anti-NMDAr	17	Seizures, Psychosis	Corticosteroids
4	Female	6	Anti-NMDAr	8	Hallucinations	None
5	Female	16	Anti-NMDAr	20	Agitation	None
6	Female	15	Anti-NMDAr	5	Seizures, Hallucinations, Psychosis	Corticosteroids, Propofol, Dexmedetomidine, Lorazepam, Anticonvulsants
7	Female	16	Hashimoto	3	Agitation, Psychosis	Olanzapine
8	Female	14	Hashimoto	7	Seizures, Ataxia	Anticonvulsants
9	Female	9	Hashimoto	8	Seizures, Hallucinations, Hemiplegia	Anticonvulsants
10	Male	2	Post Infectious Arteritis	6	Seizures, Paresis	Corticosteroids, Anticonvulsants
11	Female	6	Small vessel Arteritis	12	Seizures, Hallucination	Diamox
12	Male	6	Mycoplasma	15	Seizures, Clonism	Anticonvulsants
13	Female	2	Mycoplasma	17	Seizures, Chorea	Anticonvulsants Lorazepam (1 h30 prior to FDG)
14	Female	5	Kawasaki	3	Ataxia	None
15	Female	5	ADEM	9	Clonism	Corticosteroids, Diamox
16	Male	6	ADEM	8	Neurological deficits	Corticosteroids
17	Male	6	Viral	8	Seizures, Hallucinations	Anticonvulsants
18	Male	15	Auto-immune	4	Catatonia	None
19	Male	13	Auto-immune	3	Agitation	None
20	Male	1	Auto-immune	6	Seizures	Anticonvulsants
21	Male	7	Auto-immune	9	Seizures	Corticosteroids, Midazolam, Anticonvulsants
22	Female	3	Auto-immune	8	Seizures, Chorea	Anticonvulsants
23	Female	4	Auto-immune	5	Seizures, Ataxia	None
24	Female	1	Auto-immune	15	Seizures, Clonism	Corticosteroids, Anticonvulsants
25	Female	7	Auto-immune	4	Seizures, Hallucinations	Anticonvulsants, Quetiapine
26	Male	6	Auto-immune	6	Ataxia	Anticonvulsants, Dexmedetomidine, Propofol
27	Male	6	Auto-immune	11	Seizures, Hemiparesia	Corticosteroids, Anticonvulsants
28	Male	10	Auto-immune	5	Seizures	Anticonvulsants
29	Female	11	Lupus	6	Seizures	Corticosteroids, Anticonvulsants
30	Female	15	Lupus	2	Seizures	None
31	Female	13	Lupus	5	Ataxia	None
32	Male	2	No Diagnosis	5	Seizures	Lorazepam, (2 h prior to FDG)
33	Male	16	No Diagnosis	5	Seizures	Anticonvulsants
34	Female	10	No Diagnosis	9	Seizures	Anticonvulsants, Lorazepam

Clinical findings in addition to encephalopathy. Relevant medication includes medication that may affect brain metabolism at time of the examination. Anticonvulsants: Anticonvulsant medication without sedative effect. Delay (days) represents the delay between the hospital admission and PET

Visually assessed PET was abnormal in 32 out of 34 subjects while MRI was abnormal only in 14. In six subjects, the same diagnosis was obtained by both modalities while in the remaining 8 MRI and PET results were discordant. In some patients, diagnosis on PET and/or MRI was discordant with the final diagnosis. Subject 2 with a diagnosis of ADEM on MRI had a final diagnosis of anti-

NMDAr due to clinical presentation but without serological or CSF confirmation; subject 5 with a diagnosis of anti-NMDAr encephalitis had an abnormal MRI in keeping with encephalitis but a normal PET 3 weeks later, without treatment. Subject 11 had a diagnosis of ADEM on MRI, encephalitis on PET and final diagnosis was small vessel vasculitis; subject 13 had a diagnosis of

ischemic modifications on MRI, encephalitis on PET and the final diagnosis was an infectious process; subject 22 had a diagnosis of ADEM on MRI, encephalitis on PET and the final diagnosis was AIE. Subject 17 demonstrated anomalies in the left hippocampal region on MRI suggestive of viral encephalitis even though no pathogen was identified in the CSF (Table 2).

Altogether visually assessed PET showed anomalies in 94.1% of subjects, MRI in 41.2% and CT in 6.9%.

Distribution of PET anomalies

Visually-assessed PET was normal in two subjects (5, 15). It demonstrated a single region of abnormal uptake in six patients, three involving the temporal lobe (3, 19 and 28) and three the basal ganglia (10, 29, 31). Multiple abnormal cortical regions, with either hyper or hypometabolic foci, were found in 23 subjects involving every lobe in five. Twenty-two subjects had anomalies in the parietal lobes, 22 in the temporal lobes, 19

Table 2 PET and MRI diagnosis

Patient number	Gender	Age (years)	Qualitative PET diagnosis	MRI diagnosis	Delay (days)	Diagnostic concordance PET and MRI
1	Male	5	Encephalitis	Normal	4	No
2	Female	18	Encephalitis	ADEM	7	No
3	Female	17	Encephalitis	Normal	9	No
4	Female	6	Encephalitis	Normal	7	No
5	Female	16	Normal	Encephalitis	2	No
6	Female	15	Encephalitis	Normal	5	No
7	Female	16	Encephalitis	Normal	5	No
8	Female	14	Encephalitis	Encephalitis	17	Yes
9	Female	9	Encephalitis	Normal	7	No
10	Male	2	Vascular disease	Vascular disease	4	Yes
11	Female	6	Encephalitis	ADEM	9	No
12	Male	6	Encephalitis	Encephalitis	1	Yes
13	Female	2	Encephalitis	Ischemic modifications	1	No
14	Female	5	Encephalitis	Normal	3	No
15	Female	5	Normal	Normal	4	No
16	Male	6	Encephalitis	ADEM	14	No
17	Male	6	Encephalitis	Encephalitis	5	Yes
18	Male	15	Encephalitis	Normal	1	No
19	Male	13	Encephalitis	Normal	1	No
20	Male	1	Encephalitis	Normal	2	No
21	Male	7	Encephalitis	Normal	3	No
22	Female	3	Encephalitis	ADEM	4	No
23	Female	4	Encephalitis	Normal	5	No
24	Female	1	Encephalitis	Normal	7	No
25	Female	7	Encephalitis	Normal	0	No
26	Male	6	Encephalitis	Normal	1	No
27	Male	6	Encephalitis	Encephalitis	6	Yes
28	Male	10	Encephalitis	Normal	2	No
29	Female	11	Encephalitis	Normal	2	No
30	Female	15	Encephalitis	Normal	1	No
31	Female	13	Encephalitis	Normal	7	No
32	Male	2	Encephalitis	Anoxic encephalopathy	2	No
33	Male	16	Encephalitis	Encephalitis	5	Yes
34	Female	10	Encephalitis	Normal	4	No

Delay (days) represents the delay between MRI and PET

ADEM acute demyelinating encephalomyelitis

Table 3 Visual assessment: affected lobes with regions of hyper and/or hypometabolism and increased activity in basal ganglia

Affected lobes	Anti-NMDAr	Hashimoto's	Neurolypus	AIE /EX	Other CNS pathologies
A: Per patient					
Total number of patients	6	3	3	14	8
Frontal lobe anomalies	1	3	1	9	5
Parietal lobe anomalies	4	1	1	10	5
Temporal lobe anomalies	4	2	0	11	6
Occipital lobe anomalies	3	1	0	8	5
Basal ganglia hypermetabolism	0	1	2	5	1
B: Statistical analysis					
Frontal lobes	Anti-NMDAr	Hashimoto's	Neurolypus	AIE /EX	
Vs Hashimoto's	$p = 0.011$				
Vs Neurolypus	$p = 0.64$	$p = 0.12$			
Vs AIE /EX	$p = 0.0003$	$p = 0.51$	$p = 0.017$		
Parietal lobes	Anti-NMDAr	Hashimoto's	Neurolypus	AIE /EX	
Vs Hashimoto's	$p = 0.4$				
Vs Neurolypus	$p = 0.4$	$p = 1$			
Vs AIE /EX	$p = 0.01$	$p = 0.006$	$p = 0.006$		
Temporal lobes	Anti-NMDAr	Hashimoto's	Neurolypus	AIE /EX	
Vs Hashimoto's	$p = 1$				
Vs Neurolypus	$p = 0.07$	$p = 0.12$			
Vs AIE /EX	$p = 0.002$	$p = 0.014$	$p = 0.0001$		
Occipital lobes	Anti-NMDAr	Hashimoto's	Neurolypus	AIE /EX	
Vs Hashimoto's	$p = 0.68$				
Vs Neurolypus	$p = 0.17$	$p = 0.38$			
Vs AIE /EX	$p = 0.38$	$p = 0.04$	$p = 0.003$		
Basal Ganglia hyperactivity	Anti-NMDAr	Hashimoto's	Neurolypus	AIE /EX	
Vs Hashimoto's	$p = 0.18$				
Vs Neurolypus	$p = 0.018$	$p = 0.51$			
Vs AIE /EX	$p = 0.67$	$p = 0.32$	$p = 1$		

CNS central nervous system

in the frontal lobes and 17 in the occipital lobes (Table 3A). Posterior involvement was found in anti-NMDAr (Fig. 2). Parietal lobes were more affected in anti-NMDAr in comparison with Hashimoto's encephalitis ($p = 0.006$) (Table 3B). However, parietal lobe anomalies were also demonstrated in AIE and EX. Temporal lobes were significantly more involved in AIE/EX than in anti-NMDAr ($p = 0.002$) and Hashimoto's encephalitis ($p = 0.014$), but temporal anomalies were still present in Hashimoto's (Fig. 3). Frontal lobes anomalies were rare in anti-NMDAr when compared to AIE/EX ($p = 0.0003$). Neurolypus differed from AIE/EX for the lack of parietal, temporal, and occipital involvement ($p = 0.006$, $p = 0.0001$ and $p = 0.003$, respectively). There was a trend for less involvement of the temporal lobes in neurolypus when compared to anti-NMDAr ($p = 0.07$). Seven out of 17 patient in the neurolypus and AIE/EX groups demonstrated hypermetabolism in at least one of the basal ganglia but only one out of nine subjects with anti-NMDAr or Hashimoto's encephalitis.

Diffuse hypometabolism of the whole cortex was found in three subjects (8,13,25). Patients 8 and 25 did not received sedative medication at the time of PET and hypometabolism was discreet with preservation of basal ganglia, primary cortices and posterior fossa metabolism. Only patient 13 received Lorazepam 90 min prior to FDG administration and demonstrated reduced cortical uptake. However preserved metabolism in the basal ganglia and posterior fossa metabolism together with heterogeneous uptake in the cortex suggested that those anomalies were not secondary to sedation but rather caused by encephalitis. In the subgroup of patients receiving sedative medication at time of PET, preservation of metabolism in the basal ganglia, posterior fossa and in some gyri associated with focal defects was found. In all, while there was a tendency for posterior involvement in anti-NMDAr, more anterior anomalies in Hashimoto's encephalitis (Fig. 3) and almost exclusive basal ganglia hypermetabolism in neurolypus, there was overlap between subgroups.

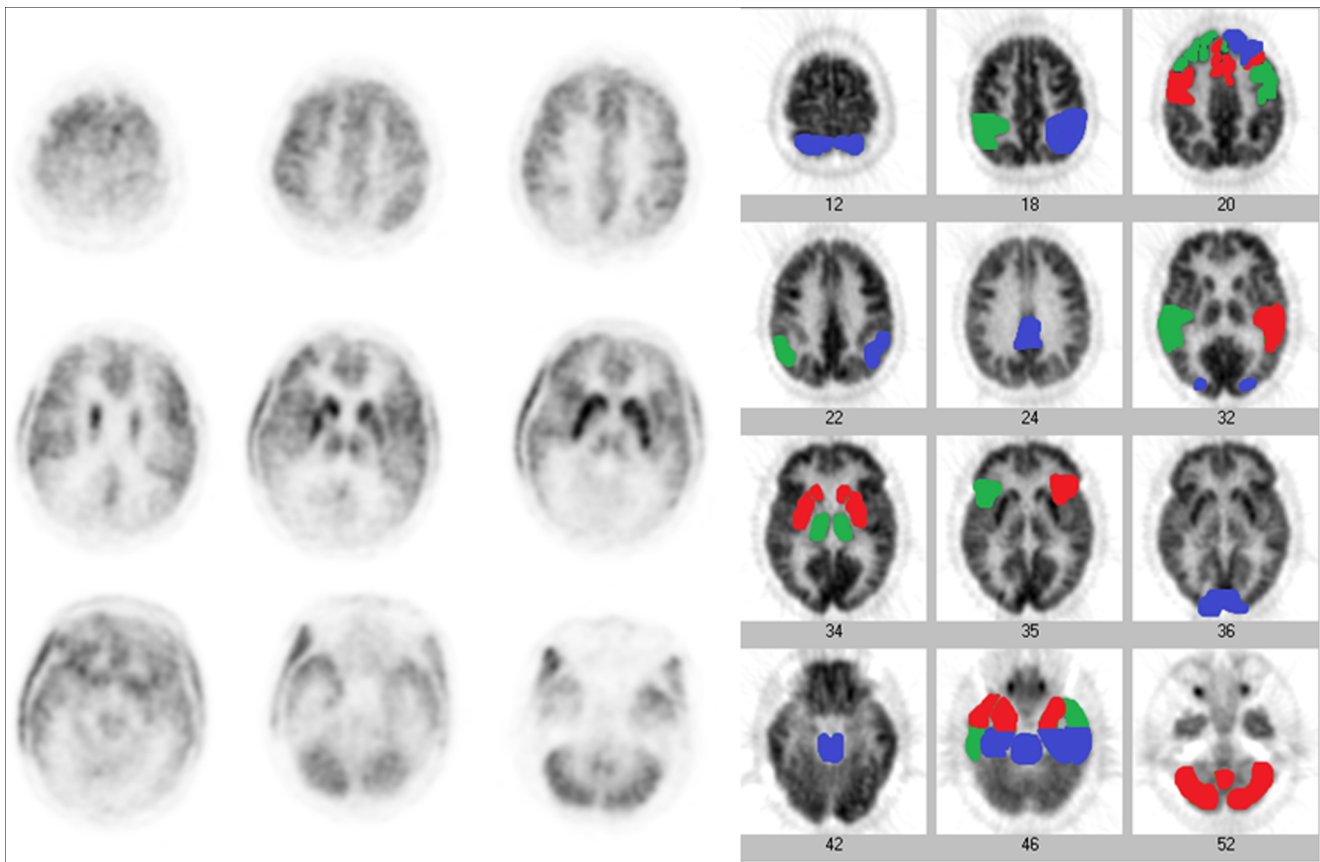


Fig. 2 Subject 6: A 13-year old girl admitted for hallucinations and delirium followed by decreased level of consciousness, seizures, dystonia and fever. Initial working diagnosis of herpes encephalitis. CSF analysis demonstrated normal protein and glucose levels, negative for viral and bacterial infection but positive for anti-NMDAr antibodies. Ultrasound of the abdomen showed an ovarian lesion which was subsequently removed and for which the pathology was in keeping with teratoma. As the patient was not improving, despite immuno-modulatory treatment and surgery and in the presence of normal brain CT and MRI, FDG PET was ordered

RRBM quantification showed at least one hypermetabolic region in 27 subjects and at least one hypometabolic region in 33. Five subjects (2,5,10,11 and 19) demonstrated only regions of decreased uptake and one patient (30) of increased uptake on PET. Basal ganglia activity was increased in 20 subjects (58.8%) with quantification, including ten out of 14 subjects with AIE or EX and all three subjects with neurolupus. Otherwise, there was no difference between the number of hypermetabolic or hypometabolic regions in either cerebral lobe or in the basal ganglia permitting the identification of each subtype of encephalitis with quantification (Table 4). However, when compared to the validation group, the number of hypermetabolic cortical regions per subject was higher in patients with encephalitis (4.09 ± 3.41 vs 0.72 ± 1.10 , $p < 0.0001$), so were the number of hypometabolic regions (8.82 ± 5.44 vs 1.66 ± 0.72 , $p < 0.0001$) and increased basal ganglia metabolism (1.56 ± 1.65 vs 0.14 ± 0.58 , $p < 0.0001$).

for reevaluation. Qualitative brain PET shows diffuse symmetrical hypometabolism, more marked in the posterior temporal, parietal and occipital lobes, with increased activity in the basal ganglia. NeuroQ™ analysis demonstrates hypermetabolism in the basal ganglia and multiple regions of relative hyper and hypometabolism, the latter predominantly in the posterior regions. NeuroQ™ analysis results overlying the adult template. *Red*: RRBM > upper limit of 95% prediction interval; *blue*: RRBM < lower limit of 95% prediction interval; *green*: RRBM within the 95% prediction interval

Follow-up

Only four subjects did not receive an immuno-modulating treatment. Despite significant functional impairment at time of presentation in most of our subjects, symptoms subsided without sequelae in 16 and with minimal sequelae in four. Five subjects developed epilepsy as complication and nine a combination of cognitive and motor impairments.

Follow-up PET, at the discretion of the referring physician, were performed in 13 subjects: six for reevaluation post treatment (1, 2, 3, 6, 24, 29), four for reevaluation of epilepsy in a pre-surgical setting (8, 12, 20 and 21) and three for evaluation of possible relapse (11, 27 and 33). There was complete normalization of PET studies performed 6–9 months later in three subjects with anti-NMDAr (1, 2, 3) and one patient with neurolupus (29) (Fig. 4). Improvement was found in three studies performed 3–15 months after the initial PET (21, 24 and 33).

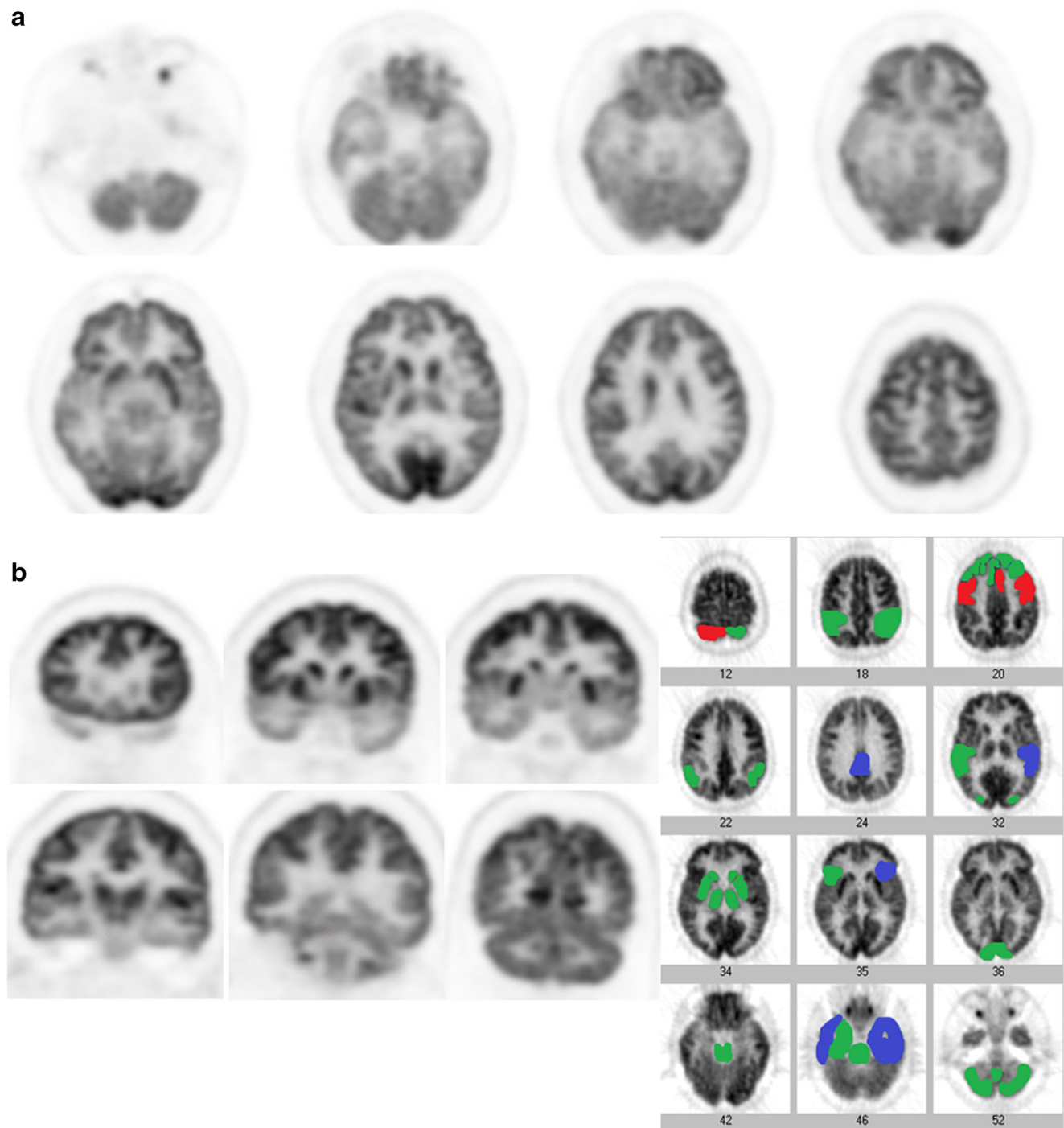


Fig. 3 Subject 8: A 16-year old girl with known Hashimoto's encephalopathy. The subject suffered from recurrent partial complex or tonic-clonic seizures, occasionally accompanied by auditory hallucinations. Initially euthyroid but with positive thyroid peroxidase antibodies ($= 152$ kIU/L; normal <6 kIU/L). The patient subsequently developed hypothyroidism. Prior to admission, her treatment included corticosteroids, anticonvulsive medication and levothyroxine. The patient was hospitalized for acute deterioration including seizures, headaches, nausea, ataxia and confusion. Blood work showed increased sedimentation rate but anti-NMDAR antibodies, anti-nuclear antibodies

and anti-DNA antibodies were negative with the exception of anti-SSA ($= 1.2$; $N < 1.0$ AI). Brain PET shows mild diffuse symmetrical hypometabolism (a), more marked in the temporal lobes (b). NeuroQ™ analysis in addition to the bilateral temporal hypometabolism, demonstrates hypermetabolism in the sensorimotor cortex and anterior cingulate. NeuroQ™ analysis results overlying the adult template. *Red*: RRBM $>$ upper limit of 95% prediction interval; *blue*: RRBM $<$ lower limit of 95% prediction interval; *green*: RRBM within the 95% prediction interval

Table 4 RRBm quantification: number of abnormal regions for each cerebral lobe and basal ganglia expressed as mean \pm SD

Increased RRBm frontal	Anti-NMDAr	Hashimoto's	NeuroLupus	AIE /EX
	1.17 \pm 2.04	1.67 \pm 1.53	0	1.79 \pm 2.58
Vs Hashimoto's	$p = 0.72$			
Vs NeuroLupus	$p = 0.37$	$p = 0.14$		
Vs AIE /EX	$p = 0.61$	$p = 0.94$	$p = 0.26$	
Decreased RRBm frontal	Anti-NMDAr	Hashimoto's	NeuroLupus	AIE /EX
	2.5 \pm 3.08	2.33 \pm 3.21	1.67 \pm 2.89	2.14 \pm 3.63
Vs Hashimoto's	$p = 0.94$			
Vs NeuroLupus	$p = 0.71$	$p = 0.80$		
Vs AIE /EX	$p = 0.84$	$p = 0.93$	$p = 0.83$	
Increased RRBm parietal	Anti-NMDAr	Hashimoto's	NeuroLupus	AIE /EX
	0.17 \pm 0.41	0.67 \pm 0.58	1 \pm 1.73	1.21 \pm 1.58
Vs Hashimoto's	$p = 0.17$			
Vs NeuroLupus	$p = 0.27$	$p = 0.77$		
Vs AIE /EX	$p = 0.13$	$p = 0.57$	$p = 0.87$	
Decreased RRBm parietal	Anti-NMDAr	Hashimoto's	NeuroLupus	AIE /EX
	2.67 \pm 2.8	3.33 \pm 1.53	2 \pm 2	2.79 \pm 2.67
Vs Hashimoto's	$p = 0.72$			
Vs NeuroLupus	$p = 0.73$	$p = 0.41$		
Vs AIE /EX	$p = 0.93$	$p = 0.74$	$p = 0.64$	
Increased RRBm temporal	Anti-NMDAr	Hashimoto's	NeuroLupus	AIE /EX
	1.67 \pm 1.86	0	1 \pm 1.73	1.64 \pm 1.5
Vs Hashimoto's	$p = 0.17$			
Vs NeuroLupus	$p = 0.62$	$p = 0.37$		
Vs AIE /EX	$p = 0.98$	$p = 0.08$	$p = 0.52$	
Decreased RRBm temporal	Anti-NMDAr	Hashimoto's	NeuroLupus	AIE /EX
	1.67 \pm 0.82	3.67 \pm 3.06	1 \pm 1	2.43 \pm 1.65
Vs Hashimoto's	$p = 0.15$			
Vs NeuroLupus	$p = 0.31$	$p = 0.22$		
Vs AIE /EX	$p = 0.30$	$p = 0.32$	$p = 0.17$	
Increased RRBm occipital	Anti-NMDAr	Hashimoto's	NeuroLupus	AIE /EX
	0.5 \pm 1.22	0	0	0.43 \pm 1.16
Vs Hashimoto's	$p = 0.51$			
Vs NeuroLupus	$p = 0.52$	None		
Vs AIE /EX	$p = 0.90$	$p = 0.54$	$p = 0.54$	
Decreased RRBm occipital	Anti-NMDAr	Hashimoto's	NeuroLupus	AIE /EX
	2 \pm 1.9	1 \pm 1.73	0.67 \pm 1.15	1.79 \pm 1.53
Vs Hashimoto's	$p = 0.47$			
Vs NeuroLupus	$p = 0.31$	$p = 0.79$		
Vs AIE /EX	$p = 0.79$	$p = 0.44$	$p = 0.25$	
Increased RRBm basal ganglia	Anti-NMDAr	Hashimoto's	NeuroLupus	AIE /EX
	1.17 \pm 1.47	2 \pm 3.46	2 \pm 2	2.43 \pm 2.14
Vs Hashimoto's	$p = 0.61$			
Vs NeuroLupus	$p = 0.75$	$p = 1$		
Vs AIE /EX	$p = 0.21$	$p = .78$	$p = 0.75$	
Decreased RRBm basal ganglia	Anti-NMDAr	Hashimoto's	NeuroLupus	AIE /EX
	0	0	0	0.07 \pm 0.27
Vs Hashimoto's	None			
Vs NeuroLupus	None	None		
Vs AIE /EX	$p = 0.66$	$p = 0.66$	$p = 0.66$	

Number of regions evaluated: 12 frontal, ten parietal, ten temporal, four occipital and six basal ganglia

Discussion

There are numerous causes of AE: infections, post-infectious, autoimmune, paraneoplastic, etc., which makes diagnosing their etiology a challenge [1–6]. For example, the California Encephalitis Project enrolled 1,570 subjects between 1998 and 2005 with AE and either confirmed or found probable etiology in only one third of cases. The larger Emerging Infections Program Encephalitis Project involved 5,000 subjects, including those of the California

Project which showed that an AE etiology was found in half of the subjects [1, 5].

AIE can be the result of an autoimmune reaction outside of the brain with subsequent transfer of autoantibodies from the blood to the brain after modification of the blood-brain barrier (BBB) or the result of an intracerebral autoimmune reaction with transfer of autoantibodies from the cerebrospinal fluid (CRF) to the blood. Antibodies present in AIE can target either intracellular or surface antigens. Antibodies directed towards intracellular antigens lead to an immune reaction

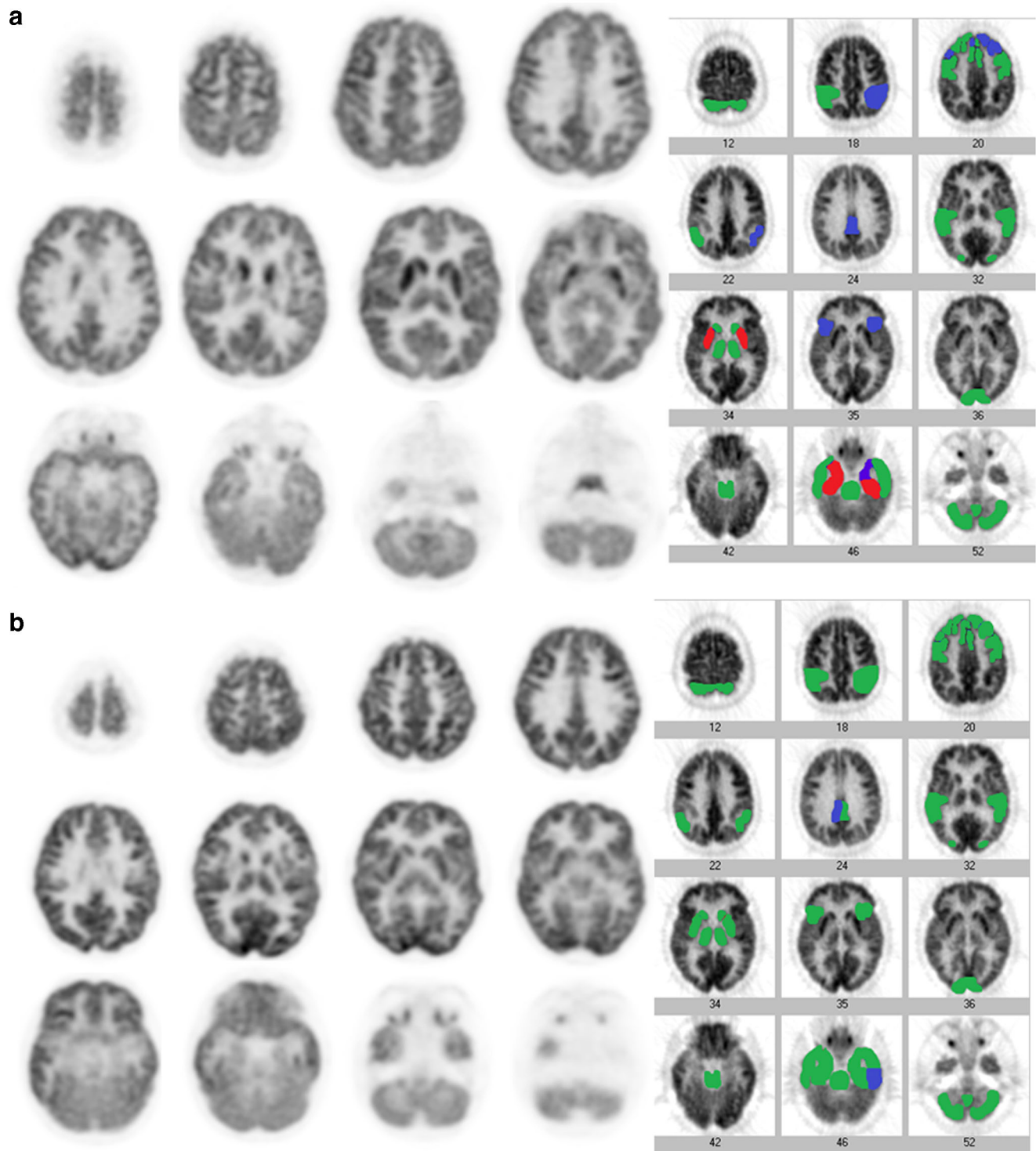


Fig. 4 Subject 29: An 11-year old girl admitted for headaches, tonic-clonic seizures, and decreased level of consciousness. The suspected diagnosis was viral encephalitis. Blood work showed increased ESR, decreased C3 and C4 values, and negative anti-NMDAr antibodies. Serological analysis revealed anti-SSA antibodies. CSF analysis showed increased protein levels and normal glucose values. Bacterial and viral PCR analysis and cultures were negative. The findings were suggestive of neurolupus and the patient was treated with anticonvulsive medication, corticosteroids and mycophenolate

mofetil. Brain PET at diagnosis showed increased uptake in the lentiform nucleus of basal ganglia. NeuroQ™ analysis demonstrates lentiform nucleus and medial temporal hypermetabolism (a). On follow-up (9 months later) neurological symptoms had subsided and qualitative brain PET was normal. NeuroQ™ analysis confirmed the hypermetabolism resolution (b). NeuroQ™ analysis results overlying the adult template. *Red*: RRBM > upper limit of 95% prediction interval; *blue*: RRBM < lower limit of 95% prediction interval; *green*: RRBM within the 95% prediction interval

mediated by CD4+ and CD8+ T cells that are able to cross the BBB. CD8+ T cell interaction through major histocompatibility complex I interferes with neuronal function. Subsequent CD4+ mediated release of cytokines, perforin and granzymes results in cell destruction. Unfortunately, T cell mediated AIE is more difficult to treat with immunomodulation [8, 10–13] than B cell mediated AIE.

Anti-NMDAr and anti-voltage gated potassium channel-complex (VGKC) are some of the receptors targeted in B cell mediated AIE. Antibody binding to surface receptors leads to their internalization and subsequent cell dysfunction. As well, inflammatory cell infiltration may be present in B cell mediated AIE. Anti-NMDAr encephalitis may be the most frequent AIE identified to date. From the California Encephalitis Project, 32 cases of anti-NMDAr encephalitis compared to 47 cases of infectious encephalitis were eventually detected in 761 subjects 30 years old and younger [14].

Our study is the first to examine the use of FDG PET in exclusively pediatric subjects with suspected AE. Our results suggest that, despite PET having a high sensitivity for metabolic abnormalities present in encephalitis, no characteristic pattern of anomalies emerged to determine the etiology of AE. In particular, we were not able to identify a pathognomonic pattern of cortical anomalies in pathologies such as anti-NMDAr encephalitis, Hashimoto's or lupus. This also applies to MRI as both modalities could not specify the subtype of encephalitis and in some patients (11, 13, 22, for example) findings mimicked other pathologies such as ischemic vascular disease, small vessel vasculitis and infection. However, basal ganglia hypermetabolism was found in a certain number of our patients and, in the appropriate clinical context, such hypermetabolism is suggestive of an auto-immune process. The central role of the basal ganglia as a target of neuro-inflammation is not new. Increased uptake on both PET and single photon emission tomography (SPECT) has been described in Sydenham chorea (SC) [15–17]. It is believed that antibodies produced during group A streptococcal infection can target not only the N-acetylglucosamine (GlcNAc) found in the bacterial cell wall but also the lysogangliosides found in the neuronal cell wall. Interaction with basal ganglia signals dopamine release and leads to subsequent choreic manifestations [17].

The anatomical distribution of metabolic abnormalities in AIE was also recently studied by others. Baumgartner et al. studied a cohort of 18 adult subjects with suspected limbic encephalitis. The clinical presentation of subacute onset of memory loss in these subjects was different than our population. MRI was abnormal in about 2/3 of cases and PET in about 3/4 of cases. Antibodies against intracellular epitopes were found in four subjects and associated with mesiotemporal anomalies on PET. Antibodies against surface antigen were found in nine subjects (6 VGKC, 2 NMDAr, 1 VGKC+NMDAr) with PET demonstrating anomalies outside the mesiotemporal regions including two subjects with striatal

hypermetabolism [18]. Solnes et al. reported findings in 23 subjects including two pediatric cases with seropositive AIE. About a quarter of the subjects had antibodies against intracellular epitopes. PET imaging was performed an average of 8 weeks after onset of symptoms. MRI was abnormal in 43% of subjects, visual PET in all subjects and quantification in 95.6%, comparable to our findings. However, only half of the subjects experienced seizures and, in all but two subjects, the duration of symptoms before presentation was 1 week or more. Basal ganglia involvement was not a predominant feature in this population. These authors reported the parietal lobes being affected in 82.6% of cases and the temporal lobes in 52.5% using quantification [19]. A more recent study in 24 subjects, including seven children, with auto-immune non-paraneoplastic encephalitis was performed by Tripathi et al. Subjects were studied on average 12 weeks after onset of symptoms and MRI was abnormal in 45.8% of cases. Sixteen subjects tested positive for anti-NMDAr antibodies and the majority demonstrated bilateral posterior hypometabolism with or without basal ganglia hypermetabolism. Some of the remaining subjects, with either anti-VGKC or anti-GAD AIE, also showed basal ganglia hypermetabolism [20]. As also stated by these authors, “the presence of basal ganglia hypermetabolism should raise the suspicion of AIE in the relevant clinical setting”. This is particularly true in a pediatric setting as other authors have reported basal ganglia hypermetabolism in children with anti-NMDAr encephalitis [21]. Posterior involvement with, in some of our patients, wedge-shaped defects in the occipital regions, was indeed demonstrated in our anti-NMDAr subjects as reported in the literature [22–24]. However, posterior anomalies were also found in some of our subjects from the AIE/EX and Hashimoto's groups and frontal anomalies in one of our anti-NMDAr subjects. Basal ganglia hypermetabolism reported in some adults with anti-NMDAr encephalitis was not found in our cohort [24]. Our findings were similar to those of the first two cases of pediatric anti-NMDAr encephalitis reported [25].

In keeping with many other studies, our results suggest that FDG PET can demonstrate abnormalities in most patients with encephalitis despite unremarkable anatomical imaging. For example, Probasco et al. performed a larger study of 61 adult subjects, including 32 in whom antibodies were identified and 17 subjects with malignancy. PET was performed an average 4 weeks after the onset of symptoms. Qualitative PET findings were not reported. Quantification showed anomalies in 85% of studies, with hypometabolism in 69%, hypermetabolism in 3% and a combination of hyper and hypo in 13%. Review of the literature done by the authors reports 139 subjects, 86% of them with abnormal PET findings, including 40% with a combination of hyper and hypometabolism, 22% with hypo only and 25% with hyper only. MRI performed in 114 subjects was abnormal in 68 [26]. This finding highlights the potential utility of PET for the evaluation of suspected encephalitis,

especially those patients without detectable abnormalities on MRI. Despite the perception of the radiation burden associated with PET imaging in the pediatric population, we believe its use is appropriate in select clinical cases with optimized imaging protocols [27].

Central nervous system involvement in systemic lupus erythematosus ranges from mild cognitive dysfunction to severe encephalitis. The severity of metabolic abnormalities on PET have been reported to be related to neurological disease severity [28]. While basal ganglia hypermetabolism has also been described, there are no pathognomonic findings of neurolyupus on PET [29]; however, whole body scanning in our subjects showed signs of systemic inflammation and lymphocytic activation in some, which may be suggestive of the diagnosis [30].

Our subjects with Hashimoto's encephalitis, also called steroid-responsive encephalopathy associated with autoimmune thyroiditis, did not show a specific pattern on brain PET [31]. However, in some of our subjects, increased uptake was found in the thyroid gland.

Our work has several limitations. Our study is retrospective and suffers the usual limitations of a study of this nature. To establish the relative sensitivities of PET and MRI, both studies would have to be performed in all subjects with suspected encephalitis. In our population, MRI always preceded PET and there was an average delay of 4.6 days between both tests. Furthermore, the poor concordance seen between the positivity rate of MRI and PET, reported in numerous studies, likely reflects the fact that patients with suspected encephalitis and negative anatomical imaging are more likely to be referred to for PET imaging compared to patients with obvious MRI abnormalities. Decision to perform the PET was at the discretion of the referring physician, most often in patients in intensive care without clear diagnosis after initial work-up or unfavorable clinical evolution after initial treatment. However, while no formal diagnostic algorithm has yet been developed, over the years, the delay between admission and PET has decreased.

Medication effects are a potential confounder. While no studies exist on the effect of midazolam in human FDG brain metabolism, diffuse decrease in whole brain FDG uptake including cerebellum has been shown following the administration of haloperidol [32], lorazepam [33], propofol and dexmedetomidine [34]. The nuclear medicine physicians interpreting the FDG brain PET paid attention to identify potential medication influence on findings and all the patients with sedative medication showed preserved activity in the posterior fossa.

Application of RRBM quantification in a pediatric clinical setting is still limited and for the time being restricted to epilepsy. A recent study compared 100 epileptic children to only 15 normal controls using SPM [35] and another created templates for age groups 6–9 year-old and 10–17 years old using

Scenium and SPM for pre-surgical mapping of epilepsy [36]. While the NeuroQ™ software has not been used by other authors in a pediatric setting, to date we have analyzed 120 normal subjects of all ages using it and our mathematical models. Our results are similar to those already published with 92.6% of regions falling in the 95% prediction interval [10].

Finally, the reference consisted of clinical diagnosis which has been shown to be difficult. It is likely that some of our subjects had anti-NMDAR encephalitis but the diagnosis could not be made at the time due to the lack of adequate testing. Final diagnosis was different from initial impression in some patients and remained elusive in others. In some cases, no diagnostic consensus could be reached between clinicians, despite an increasing armamentarium of diagnostic tests since the beginning of this study. In future years, diagnostic methods will continue to evolve with more readily available tools such as polymerase chain reaction (PCR) multiplex testing for both viruses and bacteria and biomarkers for neuronal antibodies.

While PET was not specific to identify the precise subtype of encephalitis, there was a significant difference between the patients and normal children from our validation group. One may theorize that in our cohort encephalitis was secondary to antibodies directed toward surface antigens due to the good response to immuno-modulation in most patients. PET was used in some of our subjects to evaluate treatment response and identify relapse.

Conclusion

Findings in children with AE, including AIE, differ from those in the adult population. Clinical presentation is acute, with significant encephalopathy, seizures and neuropsychiatric manifestations. In adults, presentation of AIE is usually over a period of weeks, with memory loss as the main clinical manifestation.

Almost all subjects had regions of increased FDG uptake and almost two-thirds of them basal ganglia hypermetabolism. Isolated temporal anomalies were rare. MRI imaging was normal in about half of subjects, similar to other studies. In some patients, whole body scanning helped identify the etiology of encephalitis.

Prospective studies are needed to establish the role of PET in children with suspected encephalitis in comparison with conventional imaging, its potential role for prognostication and response to therapy.

Acknowledgements Dr. Daniel H Silverman, UCLA Medical Center.

Funding This study was funded from a financial support from the Radiology, Radio-oncology and Nuclear Medicine Department, Faculty of Medicine, University of Montreal, Montreal, Quebec, Canada, "10th Faculty Competition", 2016.

Compliance with ethical standards

Ethical approval The study was approved by the ethical committee of our institution.

All procedures performed in studies involving human participants were in accordance with the ethical standards of the institutional research committee and with the 1964 Helsinki declaration and its later amendments or comparable ethical standards. For this type of study formal consent is not required.

Conflict of interest The authors declare that they have no conflict of interest.

References

- Bloch KC, Glaser CA. Encephalitis surveillance through the emerging infections program, 1997–2010. *Emerg Infect Dis.* 2015;21:1562–7.
- Falchek SJ. Encephalitis in the pediatric population. *Pediatr Rev.* 2012;33:122–33.
- Dale RC, Gorma MP, Lim M. Autoimmune encephalitis in children: clinical phenomenology, therapeutics and emerging challenges. *Curr Opin Neurol.* 2017;30:334–44.
- Graus F, Titulaer MJ, Balu R, Benseler S, Bien CG, Celluci T, et al. A clinical approach for the diagnosis of autoimmune encephalitis. *Lancet Neurol.* 2016;15:391–404.
- Venkatesan A, Tunkel AR, Bloch KC, Loring AS, Sejvar B, et al. Case definitions, diagnosis algorithms and priorities: consensus statement of the international encephalitis consortium. *Clin Infect Dis.* 2013;57:1114–28.
- Glaser CA, Honarmand S, Anderson LJ, Schnurr DP, Forghani B, Cossen CK, et al. Beyond viruses: clinical profiles and etiologies with encephalitis. *Clin Infect Dis.* 2006;43:1565–57.
- He T, Kaplan S, Kamboj M, Tang YW. Laboratory diagnosis of central nervous system infection. *Curr Infect Dis Rep.* 2016;18:35–47.
- Somner FE. Autoimmune encephalitis: history and current knowledge. Copenhagen: Statens Serum Institut; 2016. Version 5.8.
- Morbelli S, Booij J, Chen MK, Chetelat G, Cross DJ, Djekidel M, et al. On behalf of the EANM and SNMMI. The need for standardization and of large clinical studies in an emerging indication of 18F-FDG: the auto-immune encephalitis. *Eur J Nucl Med Mol Imaging.* 2017;44:353–7.
- Turpin S, Martineau PJ, Levasseur MA, Lambert R. Modeling the effects of age and gender on normal pediatric brain metabolism using 18F-FDG PET/CT. *J Nucl Med.* 2018;59:1118–24.
- Melzer N, Meuth SG, Wiendl H. Paraneoplastic and non-paraneoplastic autoimmunity to neurons in the central nervous system. *J Neurol.* 2013;260:1215–33.
- Dalmau J, Geis C, Graus F. Autoantibodies to synaptic receptors and neuronal cell surface proteins in autoimmune disease of the central nervous system. *Physiol Rev.* 2017;97:839–87.
- Pignolet BSL, Gebauer CMT, Liblau RS. Immunopathogenesis of paraneoplastic neurological syndromes associated with anti-Hu antibodies. A beneficial antitumor immune response going awry. *OncoImmunology.* 2013;2:e27384. (1–10).
- Gable MS, Sherriff H, Dalmau J, Tilleu DH, Glaser CA. The frequency of autoimmune N-methyl-D-aspartate receptor encephalitis surpasses that of individual viral etiologies in young individuals enrolled in the California encephalitis project. *Clin Infect Dis.* 2012;54:899–904.
- Erlich DJ, Walker EH. Functional neuroimaging and chorea: a systematic review. *J Clin Mov Disord.* 2017;4:8–27.
- Delle AcqueGioglio SM, Caprio MG, Galante F, Russo G, Romano A, Vergara E, et al. Clinical value of perfusion abnormalities of brain on Technetium-99m HMPAO single photon emission computed tomography in children with Sydenham chorea. *J Child Neurol.* 2017;32:316–21.
- Ho L. Hypermetabolism in bilateral basal ganglia in Sydenham chorea on 18F-FDG PET/CT. *Clin Nucl Med.* 2009;34:114–6.
- Baumgartner A, Rauer S, Mader I, Meyer PT. Cerebral FDG-PET and MRI findings in autoimmune limbic encephalitis: correlation with autoantibody types. *J Neurol.* 2013;260:2744–53.
- Solnes LB, Jones KM, Rowe SP, Pattanayak P, Nalluri A, Venkatesan A, et al. Diagnostic value of 18F-FDG PET/CT versus MRI in the setting of antibody-specific autoimmune encephalitis. *J Nucl Med.* 2017;58:1307–13.
- Tripathi M, Tripathi M, Roy SG, Parida GK, Ihtisham K, Dash D, et al. Metabolic topography of autoimmune non-paraneoplastic encephalitis. *Neuroradiology.* 2018;60:189–98.
- Lagarde S, Lepine A, Caietta E, Pelletier F, Boucrot J, Chabrol B, et al. Cerebral 18 FluoroDeoxyglucose positron emission tomography in paediatric anti N-Methyl-D-aspartate receptor encephalitis: a case series. *Brain and Development.* 2016;38:461–70.
- Probasco JC, Solnes L, Nalluri A, Cohen J, Jones KM, Zan E, et al. Decreased occipital lobe metabolism by FDG PET/CT: an anti-NMDA receptor encephalitis biomarker. *Neurol Neuroimmunol Neuroinflamm.* 2018;5:e413–9.
- Leyboldt F, Buchert R, Kleiter I, Mariehagen J, Gelderblom M, Magnus T, et al. Fluorodeoxyglucose positron emission tomography in anti-Nmethyl-D-aspartate receptor encephalitis; distinct pattern of disease. *J Neurol Neurosurg Psychiatry.* 2012;83:681–6.
- Yuan J, Guan H, Zhou X, Niu N, Li F, Cui L, et al. Changing brain metabolism patterns in subjects with ANMDARE: serial 18F-FDG PET/CT findings. *Clin Nucl Med.* 2016;41:1–5.
- Pillai SC, Gill D, Webster R, Howman-Giles R, Dale RC. Cortical hypometabolism demonstrated by PET in relapsing NMDA receptor encephalitis. *Pediatr Neurol.* 2010;43:218–20.
- Probasco JC, Solnes L, Nalluri A, Cohen J, Jones KM, Zan E, et al. Abnormal brain metabolism on FDG-PET/CT is a common early finding in autoimmune encephalitis. *Neurol Neuroimmunol Neuroinflamm.* 2017;4:e352. (1–10). <https://doi.org/10.1212/NXI.0000000000000352>.
- Strauss J, Franzius C, Pfluger T, Juergens KU, Biassoni L, Begent J, et al. Guidelines for 18F-FDG PET and PET-CT imaging in paediatric oncology. *Eur J Nucl Med Mol Imaging.* 2008;35:1581–8.
- Weiner SM, Otte A, Schumacher M, Klein R, Gutfleisch J, Brink I, et al. Diagnosis and monitoring of central nervous system involvement in systemic lupus erythematosus: value of 18F-Fluorodeoxyglucose PET. *Ann Rheum Dis.* 2000;59:377–85.
- Lee SW, Park MC, Lee SK, Park YB. The efficacy of brain 18F-fluorodeoxyglucose positron emission tomography in neuropsychiatric lupus subjects with normal brain magnetic resonance imaging findings. *Lupus.* 2012;21:1531–7.
- Nowak M, Carrasquillo JA, Yarboro CH, Bacharach SL, Whitley M, et al. A pilot study of the use of FDG PET to assess the distribution of activated lymphocytes in subjects with SLE. *Arthritis Rheum.* 2004;50:1233–8.
- Pari E, Rinaldi F, Premi E, Codella M, Renata R, Paghera B, et al. A follow-up 18F-FDG brain PET study in a case of Hashimoto's encephalopathy causing drug-resistant status-epileptic treated with plasmapheresis. *J Neurol.* 2014;261:663–7.
- Bartlett EJ, Brodie JD, Simkowitz P, Dewey SL, Rusinek H, Wolf AP, et al. Effects of haloperidol challenge in regional glucose utilization in normal human subjects. *Am J Psychiatry.* 1994;151:681–8.
- Wang GJ, Volkow ND, Fowler JS, Hitzemann RJ, Pappas NR, Netuzil N. Evaluation of gender differences in regional brain

- metabolic responses to lorazepam. *Psychiatry Res (Neuro)*. 1998;82:37–47.
34. Laaksonen L, Kallioinene M, Långsjö J, Laitio T, Scheinin A, Scheinin J, et al. Comparative effects of dexmedetomidine, propofol, sevoflurane, and S-ketamine on the regional cerebral glucose metabolism in humans: a positron emission tomography study. *Br J Anaesth*. 2018;121:281–90.
 35. Zhu Y, Feng J, Wu S, Hou H, Ji J, Zhang K, et al. Glucose metabolic profile by visual assessment combined with statistical parametric mapping analysis in pediatric patients with epilepsy. *J Nucl Med*. 2017;58:1293–9.
 36. De Blasi B, Barnes A, Galazzo IB, Hua CH, Shulkin B, Koepp M, et al. Age-specific 18F-FDG image processing pipelines and analysis are essential for individual mapping of seizure foci in paediatric patient with intractable epilepsy. *J Nucl Med*. 2018;59:1590–6.

Publisher's note Springer Nature remains neutral with regard to jurisdictional claims in published maps and institutional affiliations.